文章编号：1006-9941(2017)10-0829-09

Synthesis, Crystal Structure and Thermal Decomposition of Triaminoguanidinium 2,4,6-Trioxo-1,3,5-triazinan-1-ide Based on Cyanuric Acid

LIU Qiang-qiang[1,2], JIN Bo[2], ZHANG Qing-chun[2], SHANG Yu[2], GUO Zhi-cheng[3], PENG Ru-fang[1,2]

(1. *Research Center of Laser Fusion, China Academy of Engineering Physics, Mianyang* 621999, *China*; 2. *State Key Laboratory Cultivation Base for Nonmetal Composites and Functional Materials, Southwest University of Science and Technology, Mianyang* 621010, *China*; 3. *School of National Defence Science and Technology, Southwest University of Science and Technology, Mianyang* 621010, *China*)

Abstract: A nitrogen-rich energetic compound—triaminoguanidinium 2,4,6-trioxo-1,3,5-triazinan-1-ide (**1**) was prepared with a yield of 91% via one-step metathesis reaction using triaminoguanidinium hydrochloride (TAG-HCl) and sodium cyanurate (CANa) as raw materials. The structure of the product was characterized by X-ray single-crystal diffraction, UV-Vis, FT-IR, ^{1}H NMR, mass spectrometry and elemental analysis. The enthalpy of formation and detonation parameters of the product were calculated. Its thermal stability, non-isothermal reaction kinetics and decomposition process were studied by differential scanning calorimetry (DSC) at a heating rate of 10 K·min^{-1} and thermogravimetric (TG) analysis coupled with Fourier transform infrared spectroscopy (FTIR). The impact sensitivity of the product was determined by the drop hammer test. Results show that the crystal of compound **1** is monoclinic, space group $P2_1/n$ with a calculated density of 1.676 g·cm^{-3}. Its enthalpy of formation is 327.9 kJ mol^{-1}, the detonation velocity 7900 m·s^{-1}, and the detonation pressure 26.5 GPa. Probable thermal decomposition mechanism of **1** under N_2 atmosphere as shown in the text is proposed. Compound **1** is very insensitive to impact, and the impact sensitivity is greater than 60 J, which is better than that of TATB (50 J).

Key words: triaminoguanidinium 2,4,6-trioxo-1,3,5-triazinan-1-ide; cyanuric acid (CA); single crystal structure; ionic salt; kinetics; thermal decomposition

CLC number: TJ55; O62 **Document code**: A **DOI**: 10.11943/j.issn.1006-9941.2017.10.007

1 Introduction

As a significant branch of material science, energetic materials including explosives, propellants, and pyrotechnics, continue to be an intensively investigated area of the utmost importance. It is the key goal for scientists to find new energetic materials with high explosive performance, low sensitivity and good chemical and thermal stability[1-2]. High nitrogen heterocycle energetic materials (EMs) have drawn much attention of researchers for the increased crystalline density, positive enthalpy of formation, high thermal stability and low sensitivity to impact and friction[3-8]. Compared with traditional energetic materials, new nitrogen heterocyclic energetic compounds, such as azoles, triazines etc. which contain large numbers of N—N and C—N bonds, high heats of formation and aromatic π bond structure, are considered to be the most promising compounds[6-13]. Their derivatives can be used as gas generating agents, propellants and pyrotechnics, and have been investigated intensively[2,14-17].

Because of its good stability, high nitrogen content (51.83%), and positive heat of formation, 1,3,5-triazine, a six-membered ring heterocycle with alternating C—N bonds, is a potential building block for emerging energetic compound. A series of derivatives of *s*-triazines containing energetic substituents were investigated through amination[18-19], hydroxylation[12,20-22], azidation[23-26] and nitration[13,27-28] etc. Although these compounds are highly energetic due to their positive heats of formation, the characteristics of high sensitivity significantly limit their application potential for use on a large scale.

Since the first guanidine derivative was prepared as early as 1866, guanidine chemistry has evolved into an extremely wide-ranging field of application from bioorganic chemistry and biochemistry to inorganic chemistry and material chemistry[29-30]. In recent years, the development of new high-energy-density materials has focused on seeking environmentally high-nitrogen-content compounds. Various high-nitrogen-con-

Received Date: 2017-03-30; **Revised Date**: 2017-06-13

Project Supported: National Natural Science Foundation of China (51372211), Open Project of State Key Laboratory Cultivation Base for Nonmetal Composites and Functional (14tdfk05), Southwest University of Science and Technology Outstanding Youth Fundation (13zx9107).

Biography: LIU Qiang-qiang (1987-), male, Ph. D, research field: the synthesis of energetic materials, e-mail: liuqq87@163.com

Corresponding Author: JIN Bo (1982-), male, professor, major in synthesis and property of energetic materials, e-mail: jinbo0428@163.com;

PENG Ru-fang (1967-), female, professor, research field: fullerene chemistry and the synthesis and property of energetic materials, e-mail: rfpeng2006@163.com

tent energetic salts including full series of the guanidinium cations have been investigated[24,31].

In our previous reports[32], a series of energetic salts based on cyanuric acid (CA) were synthesized. But there are no single crystal report and systematic investigations on triaminoguanidinium which maybe have potential applications as an energetic material. In this work, both its theoretical and experimental investigations were carried out, such as the heat of formation, detonation velocity, detonation pressure, thermal stability, decomposition process, non-isothermal kinetic analysis and so on. All indicated that this salt is a potential and impact insensitive energetic material.

2 Experimental

Caution! Triaminoguanidinium 2,4,6-trioxo-1,3,5-triazinan-1-ide (**1**) is an energetic compound. Though, it has not exploded or detonated in the course of this research, this material should be handled with extreme care by using the best safety practices.

2.1 Materials and Instruments

Triaminoguanidine hydrochloride was prepared according to reference, and other reagents were purchased from commercial sources. FT-IR spectra were recorded on a Nicolet 380 FT-IR spectrophotometer (Thermo Fisher Nicolet, USA) employing a KBr matrix with a resolution of 4 cm^{-1}, in the wavelength range of 400 cm^{-1} to 4000 cm^{-1}. ^1H NMR spectra were obtained in DMSO-d_6 on a JEOL GSX 600 MHz nuclear magnetic resonance (NMR) spectrometer by using tetramethylsilane as an internal standard. Elemental analysis was performed on a Vario ELCUBE (Germany) Elemental Analyzer. DSC was performed by a Q200 DSC instrument (TA Instruments, United States) at a heating rate of 5, 10, 15 K·min^{-1} and 20 K·min^{-1} in flowing high-purity nitrogen. TGA was performed with an SDT Q600 TGA instrument (TA Instruments, United States) at a heating rate of 10 K·min^{-1} in flowing high-purity nitrogen.

2.2 Synthesis and Characterization of 1

Firstly, CA (1.29 g, 10.0 mmol), NaOH (1.22 g, 30.5 mmol) and distilled water (15 mL) were added to a 50 mL eggplant-shaped flask. And the mixture was stirred at room temperature until the solid completely dissolved, to obtain a colorless transparent solution. After removal of water under vacuum, the precipitate was filtered off, and washed three times with chilled ethanol (5 mL) to remove small amounts of NaOH. The product was then dried in a vacuum oven at 50℃, yielding white powder 2.25g (90.4%).

Next, CANa solution (0.195 g, 1.0 mmol, 1.5 mL distilled water) was slowly added dropwise totriaminoguanidine hydrochloride solution (0.422 g, 3.0 mmol, 4 mL distilled water) under stirring. Then the addition was completed and precipitation appeared, and the resulting suspension was stirred for 2 h at room temperature. The precipitated was filtered off, and washed four times (ice-water, 1.5 mL × 2; chilled ethanol 1.5 mL×2). Product was freeze-dried to give a white powder 0.21 g, yield 91%, and recrystallized from distilled water to give colorless needles (no melting point, T_{dec} = 538.9 K, DSC, N_2 atmosphere, 10 K·min^{-1}). UV-Vis (H_2O): λ_{max} =215 nm; FT-IR (KBr, ν/cm^{-1}): 3535, 3449, 3320, 3212, 2836, 1747, 1656, 1601, 1486, 1386, 1334, 1127, 1086, 950, 783, 557; ^1H NMR (DMSO-d_6, 600 MHz) δ: 4.47 (s, 9H, NH—NH_2), 9.18 (s, 2H, NH) pp; MS (ESI) m/z: 234.3 $(M+H)^+$; Elemental analysis ($C_4H_{11}N_9O_3$, %) Calcd: C 20.60, H 4.72, N 54.08; Found: C 20.69, H 3.75, N 54.72.

3 Results and Discussion

3.1 Synthesis

Cyanuric acid (CA) was reacted with NaOH to get its sodium salts (CANa), and then the salt (**1**) was synthesized by reaction of CANa and triaminoguanidine hydrochloride (TAG-HCl). Synthesis route is shown in Scheme 1. Both CANa and TAG-HCl have excellent solubility in water, and the obtained product after their mixing is precipitation, which can be filtered off to get white solid. The salt was recrystallized from distilled water to give colorless needles, and it does not seem to be hydroscopic and could be stored for years based on comparison of the DTA, DSC and TG of the original sample and the sample which stored in the open and humid environment (ambient humidity from 50% to 60%) for one year.

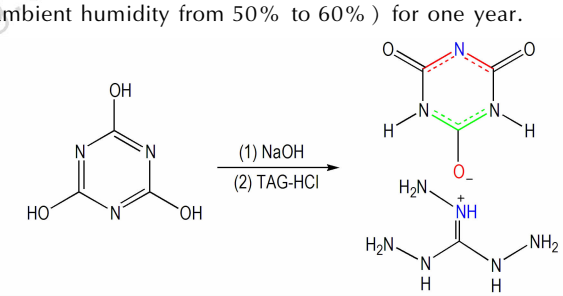

Scheme 1 Synthetic route of **1**

3.2 Crystal Structure

Single crystal of **1** was mounted on a glass fiber. All measurements were performed on a Smart Apex CCD diffractometer (Bruker) equipped with graphite monochromatized Mo-Kα radiation (λ = 0.71073 Å) using the ω and φ scan mode. The structure was solved by direct methods using SHELXS-97[33] and refined by means of full-matrix least-squares procedures on F^2

with the SHELXL-97 program[34]. All non-H atoms were located using subsequent Fourier-difference methods and refined anisotropically. In all cases, hydrogen atoms were placed in their calculated positions and thereafter allowed to ride on their parent atoms. Selected data and parameters from the X-ray data collection and refinement are given in Table 1. Further information regarding the crystal-structure determination has been deposited with the Cambridge Crystallographic Data Centre (CCDC) as supplementary publication No. 1498998.

Table 1 Crystallographic data and structure refinement parameters of **1**

formula	$C_4H_{11}N_9O_3$
mass	233.22
crystal color	colorless
crystal system	Monoclinic
space group	$P2_1/c$
a/Å	11.552(2)
b/Å	11.556(2)
c/Å	7.1471(15)
α/(°)	90
β/(°)	104.316(4)
γ/(°)	90
V/Å^3	924.4(3)
Z	4
T/K	150(2)
λ/Å	0.71073
D_c/g·cm^{-3}	1.676
μ/mm^{-1}	0.156
F(000)	488
crystal size	0.20 mm×0.19 mm×0.18 mm
θ/(°)	2.53 to 25.01
No. Refl. collected	4581
No. Indep. reflections	1630
[R_{int}]	0.0388
GOF on F^2	1.006
final R indices [$I>2\sigma(I)$]	R_1=0.0419, wR_2=0.1187
R indices (all data)	R_1=0.0535, wR_2=0.1249

Note: GOF = Goodness of Fit; $R_1 = \sum \| F_o \| - \| F_c \| / \sum \| F_o \|$; $wR_2 = [(w(F_o^2-F_c^2)^2)/w(F_o^2)^2]^{1/2}$

The X-ray crystallographic analysis data for **1** shows that the crystal is monoclinic, space group $P2_1/c$ with a calculated density of 1.676 g·cm^{-3} based on four molecules packed in the unit-cell volume of 924.4(3) Å^3. The molecular moiety is shown in Fig. 1.

The bond lengths in the triaminoguanidinium cation correspond exactly to the values observed for triaminoguanidinium nitrate and triaminoguanidinium dinitramide[35]. Because of the negative charge on anion ring, all the C—N bonds and C—O bonds of anion are slightly changed, which were compared with the structure of CA·H_2O. The bond lengths of C(2)—N(7) [1.348(3) Å], C(2)—N(9) [1.382(3) Å], C(3)—N(7) [1.341(3) Å], C(3)—N(8) [1.382(3) Å], C(4)—N(8) [1.357(3) Å] and C(4)—N(9) [1.354(3) Å] are between standard C—N single bond (1.47 Å) and standard C═N double bond (1.32 Å) lengths and are indicative of an aromatic system[32, 37-38]. The C(2)—O(1) [1.243(3) Å], C(3)—O(2) [1.243(3) Å] and C(4)—O(3) [1.224(3) Å] bond lengths are longer than the standard C═O [1.215 Å] double bond[32], indicating the CA^- anion ring tautomerism.

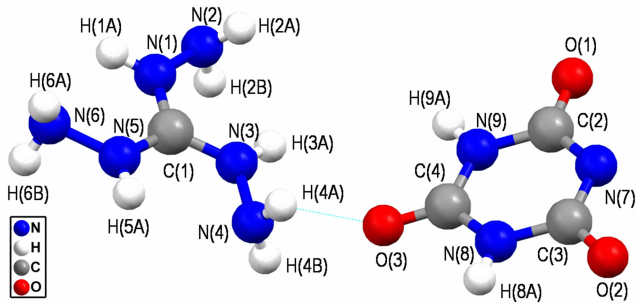

Fig. 1 Ball-and-stick molecular unit of **1**

In addition, the bond angles of nitrogen heterocyclic in the range of 114.2(2)°–124.88(17)° are closed to 120°, which further confirm tautomerism of *s*-triazines ring. Meanwhile, all the torsion angles [i.e. N(1)—C(1)—N(3)—N(4) (–178.6°), O(2)—C(3)—N(7)—C(2) (–179.61°), O(3)—C(4)—N(8)—C(3) (179.10°), N(8)—C(3)—N(7)—C(2) (0.5°)] are close to ±180° and 0°, which illustrates atoms of anion are coplanar. All bond lengths and angles are consistent with our previous reports[32].

The packing of **1** is characterized by a 3D network, which is built by twelve different hydrogen bonds. All hydrogen atoms of the cations and anions, as well as the oxygen atoms and N(7) of the anions, and N(2), N(4) of cations participate in these bridges (Fig. 2a). As shown in Fig. 2a, hydrogen bonds can be roughly divided into three kinds, one exists in two cations, another one is formed between anions and cations, and the last one is located in anions with anions. Its packing structure is configured by hydrogen bonds; the extensive hydrogen-bonding interactions form a complex 3D network (Fig. 2b). Further details about bond length, bond angle, torsion angle and hydrogen bonds are provided in Table 2– Table 4.

Table 2 Some bond lengths and angles of **1**

bond	length/Å	bond	angle/(°)
O(1)—C(2)	1.243(3)	N(5)—C(1)—N(3)	120.51(19)
O(2)—C(3)	1.243(2)	N(5)—C(1)—N(1)	119.48(18)
O(3)—C(4)	1.224(3)	N(3)—C(1)—N(1)	120.02(18)
C(1)—N(5)	1.321(3)	O(1)—C(2)—N(7)	122.4(2)
C(1)—N(3)	1.324(2)	O(1)—C(2)—N(9)	117.99(19)
C(1)—N(1)	1.326(3)	N(7)—C(2)—N(9)	119.56(19)
C(2)—N(7)	1.348(3)	O(2)—C(3)—N(7)	122.31(19)
C(2)—N(9)	1.382(3)	O(2)—C(3)—N(8)	117.89(19)
C(3)—N(7)	1.341(3)	N(7)—C(3)—N(8)	119.80(19)
C(3)—N(8)	1.382(3)	O(3)—C(4)—N(9)	123.1(2)
C(4)—N(9)	1.354(3)	O(3)—C(4)—N(8)	122.6(2)
C(4)—N(8)	1.357(3)	N(9)—C(4)—N(8)	114.2(2)
N(1)—N(2)	1.401(2)	C(1)—N(1)—N(2)	124.88(17)
N(3)—N(4)	1.408(2)	C(1)—N(3)—N(4)	119.52(17)
N(5)—N(6)	1.411(2)	C(1)—N(5)—N(6)	117.49(18)
		C(3)—N(7)—C(2)	118.97(19)
		C(4)—N(8)—C(3)	123.62(19)
		C(4)—N(9)—C(2)	123.77(18)

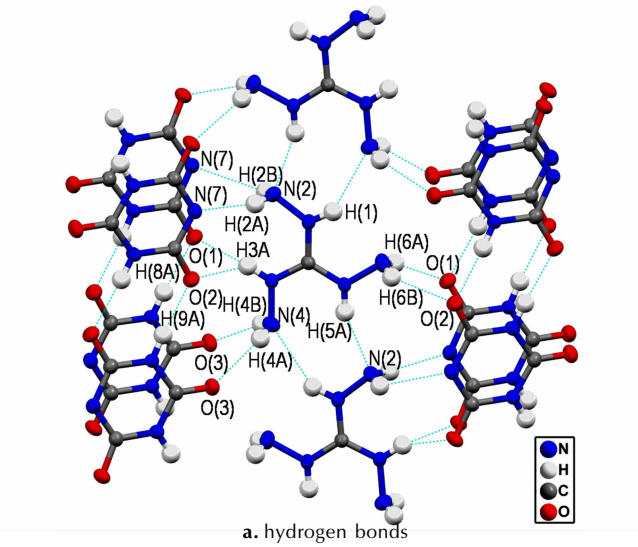

a. hydrogen bonds

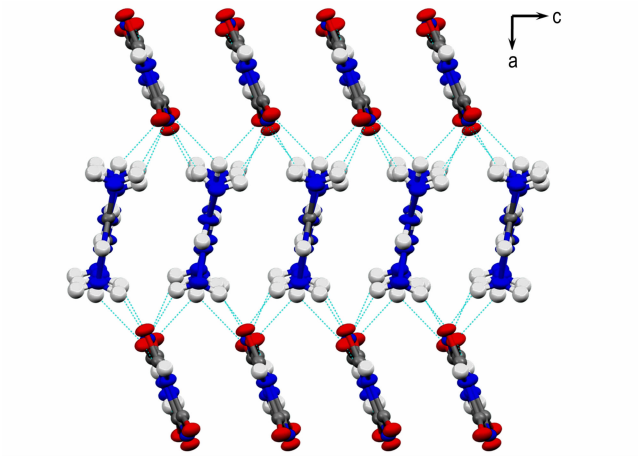

b. packing diagram viewed down the *b* axis

Fig. 2 Hydrogen bonds and packing diagram of **1** (Dashed lines indicate hydrogen bonding)

Table 3 Torsion angles of **1**

bond	angle/(°)
N(5)—C(1)—N(1)—N(2)	174.7(2)
N(3)—C(1)—N(1)—N(2)	−5.5(3)
N(5)—C(1)—N(3)—N(4)	1.2(3)
N(1)—C(1)—N(3)—N(4)	−178.6(2)
N(3)—C(1)—N(5)—N(6)	177.61(19)
N(1)—C(1)—N(5)—N(6)	−2.6(3)
O(2)—C(3)—N(7)—C(2)	−179.61(19)
N(8)—C(3)—N(7)—C(2)	0.5(3)
O(1)—C(2)—N(7)—C(3)	−178.3(2)
N(9)—C(2)—N(7)—C(3)	1.1(3)
O(3)—C(4)—N(8)—C(3)	179.10(19)
N(9)—C(4)—N(8)—C(3)	0.2(3)
O(2)—C(3)—N(8)—C(4)	178.89(19)
N(7)—C(3)—N(8)—C(4)	−1.2(3)
O(3)—C(4)—N(9)—C(2)	−177.4(2)
N(8)—C(4)—N(9)—C(2)	1.4(3)
O(1)—C(2)—N(9)—C(4)	177.24(19)
N(7)—C(2)—N(9)—C(4)	−2.2(3)

Table 4 Hydrogen bonds of **1**

D—H···A	*d*(D—H) /Å	*d*(H···A) /Å	*d*(D···A) /Å	∠(DHA) /(°)
N(1)—H(1A)···N(4)#1	0.88	2.404	3.158	143.82
N(2)—H(2B)···N(7)#2	0.863	2.539	3.112	124.69
N(2)—H(2A)···N(7)#3	0.857	2.221	3.043	160.75
N(3)—H(3A)···O(1)#2	0.88	2.266	3.037	146.19
N(3)—H(3A)···O(2)#3	0.88	2.482	3.026	120.56
N(4)—H(4B)···O(3)#4	0.863	2.206	2.974	148.25
N(4)—H(4A)···O(3)#5	0.86	2.182	2.918	143.43
N(5)—H(5A)···N(2)#6	0.88	2.149	2.984	158.01
N(6)—H(6B)···O(2)#7	0.861	2.328	3.043	140.62
N(6)—H(6A)···O(1)#8	0.859	2.305	3.11	156.2
N(8)—H(8A)···O(1)#9	0.88	1.953	2.831	175.32
N(9)—H(9A)···O(2)#2	0.88	1.938	2.815	174.53

Note: Symmetry transformations used to generate equivalent atoms: #1 $-x+1$, $y-1/2$, $-z+1/2$; #2 $-x+2$, $y+1/2$, $-z+1/2$; #3 $-x+2$, $-y+1$, $-z+1$; #4 x, $y+1$, z; #5 x, $-y+3/2$, $z+1/2$; #6 $-x+1$, $y+1/2$, $-z+1/2$; #7 $x-1$, $y+1$, z; #8 $x-1$, $-y+3/2$, $z-1/2$; #9 $-x+2$, $y-1/2$, $-z+1/2$.

3.3 Thermal Stability and Thermal Decomposition

Approximately 2.5 mg of the salt was tested at 10 K·min^{-1} to determine the melting point (T_m) and decomposition temperature (T_{dec}). As shown in Fig. 3, There is no melting endothermic peak and only one exothermic process (decomposition) peak at 538.9 K in the DSC curve (350–650 K).

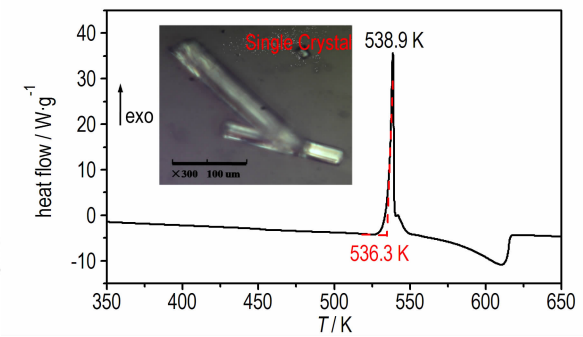

a. single crystals

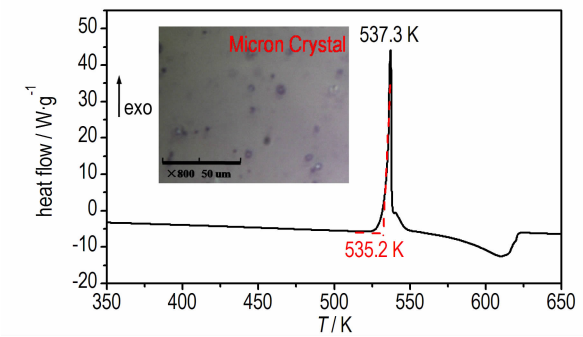

b. micron crystals

Fig. 3 DSC curves of **1** at a heating rate of 10 K·min^{-1} under nitrogen atmosphere

The relevant exothermic enthalpy change of **1** is about 100 kJ · mol^{-1} and the decomposition peak temperature is 538.9 K with extrapolated onset temperature (T_{onset}) at 536.3 K. The narrow and sharp peak indicates the decomposition of **1** is rapid decomposition and the value of T_{dec} is higher than that of RDX (513.2 K, same test conditions) and CL-20 (521.0 K, same test conditions). Therefore, as a potential energetic material, this salt possesses sufficient thermal stability.

In order to well understand the thermal decomposition behavior of **1**, the decomposition process of the salt was also investigated. Fig. 4 shows that the decomposition process of the compound can be divided into two steps roughly, and the total mass loss is greater than 95% when the temperature was heated to 873.2 K. The first process in the range of 517.5 K to 567.3 K was inferred as the loss of TAG^+ cations (observed 44.3%, calculated 45.0%). The second step from 567.3 K to 870.2 K was considered as the decomposition of anions (observed 51.5%, calculated 54.9%).

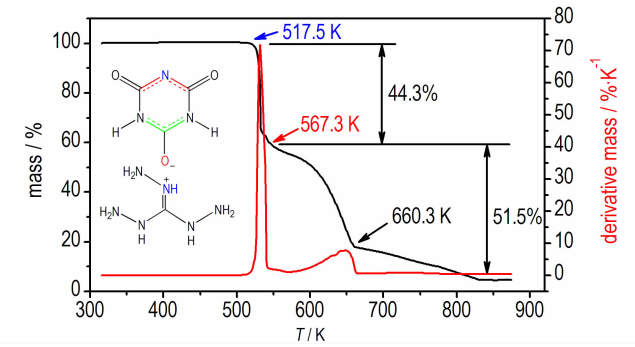

Fig. 4 TG-DTG curve of **1** at a heating rate of 10 K · min^{-1} under nitrogen atmosphere

Thermogravimetric analysis tandem infrared spectrum was used to rapidly identify the constituents of the thermal decomposition gas. Fig. 5 and Fig. 6 show the infrared spectra of gas products during decomposition at different temperatures and gas intensity at different times, respectively. From Fig. 5, we can see the decomposition processes of **1**:

Firstly, the temperature at 515.2 K, the salt did not decompose, and there was no infrared spectrum absorption.

Secondly, the temperature at 520.2 K, infrared spectrum absorption of NH_3 at 960 cm^{-1} and 930 cm^{-1} appeared. Then with the increase of temperature, absorption peaks of NH_3 at 1626 cm^{-1} and 3334 cm^{-1} arose, and the maximum absorption intensity existed at 533.2 K. Meanwhile, there was also an appearance of HCN absorption peaks at 2310 cm^{-1} and 2348 cm^{-1}.

Thirdly, infrared spectrum absorptions of NH_3 and HCN disappeared gradually, and when the temperature was heated to 585.2 K, the peaks of CO appeared and got its maximum absorption intensity at 638.2 K. Then, the absorption is gradually reduced to disappear with the temperature rising.

According to the structure of salt and decomposition gas infrared spectrum data, the probable decomposition mechanism can be deduced as Fig. 7.

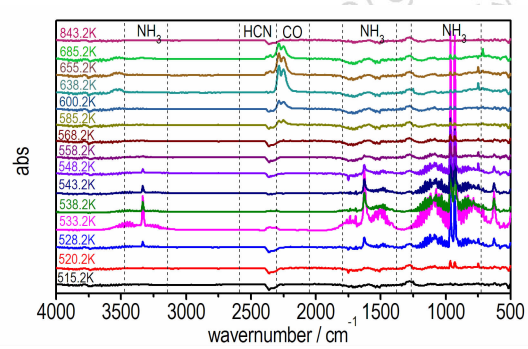

Fig. 5 FT-IR spectra of gas products of **1** during decomposition at different temperatures

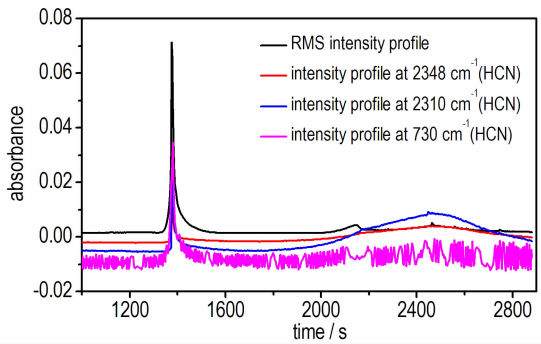

a. HCN intensity

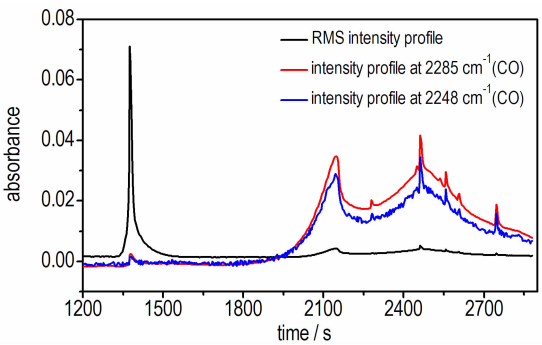

b. CO intensity

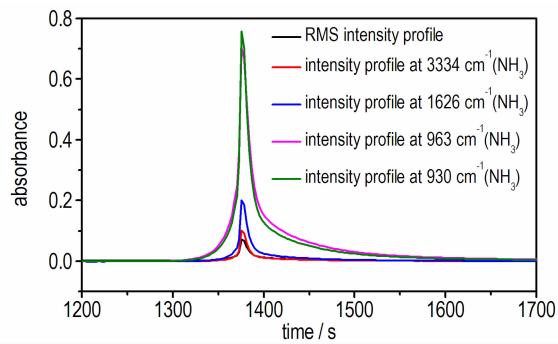

b. NH_3 intensity

Fig. 6 Thermal decomposition gas intensities at different time

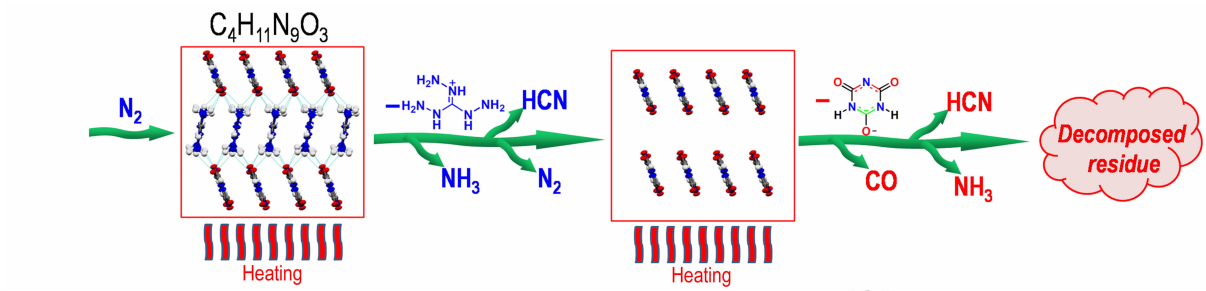

Fig. 7 Probable thermal decomposition mechanism of **1** under N_2 atmosphere

3.4 Non-isothermalKinetic Analysis

Kissinger's[41] and Ozawa's methods[42-43] were used to determine the kinetics parameters based on the exothermic peaks temperature determined from DSC curves with four different heating rates (5, 10, 15, 20 K · min^{-1}; Fig. 8). The Kissinger eqn. (1) and Ozawa-Doyle eqn. (2) are as follows:

$$\ln[\beta/T_p^2] = \ln[AR/E] - [E/RT_p] \quad (1)$$

$$\ln\beta = C - 0.4567E/RT \quad (2)$$

where β is the heating rate, K · min^{-1}; T_p is the peak temperature, K; A is the pre-exponential factor, s^{-1}; E is the apparent activation energy, kJ · mol^{-1}; and R is the gas constant (8.314 J · K^{-1} · mol^{-1}).

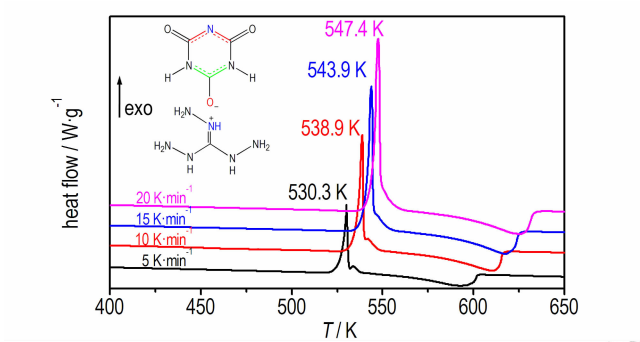

a. single crystals

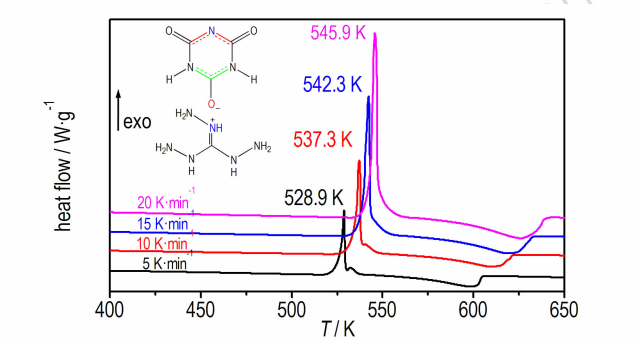

b. micron crystals

Fig. 8 DSC curves of **1** at different heating rates under N_2 atmosphere

The apparent activation energies (E), pre-exponential factors (A), and linear correlation coefficients (r) were calculated by using the values of peak temperature, Kissinger equation and Ozawa—Doyle equation. The results were summarized in Table 5. Linear relationships of ln (β/T_{p2}) and lnβ vs 1/T_p are shown in Fig. 9 and the linear correlation coefficients are very close to 1, demonstrating that the results are credible.

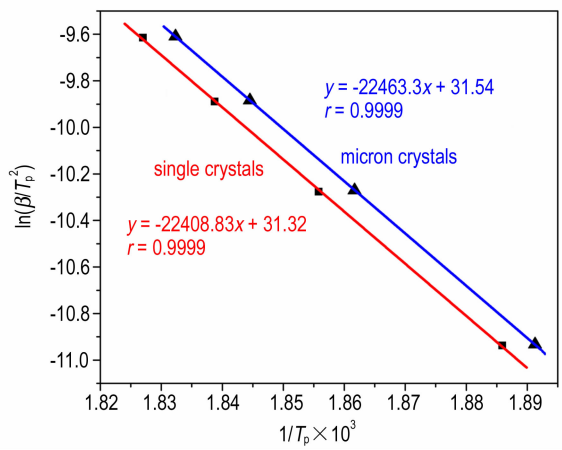

a. Kissigner method

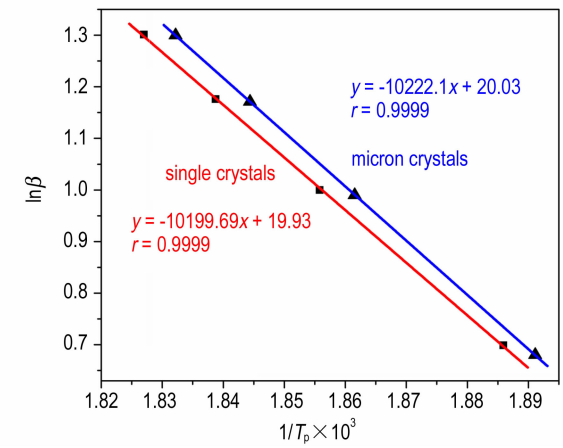

b. Ozawa method

Fig. 9 Linear relationship of ln (β/T_p^2) vs 1/T_p and lnβ vs 1/T_p of **1**

From Fig. 8 and Table 5, it can be seen that the exothermic peaks shift to higher temperatures as the heating rate increases and the T_p of micron crystals (about 5 μm) is lower (about 1.5 K) than that of single crystals. The results show

that the crystals size has little influence on E, and both of E values are approx. 186 kJ mol^{-1}, which are higher than that of RDX (about 142 kJ · mol^{-1})[39], and close to CL-20 (about 190 kJ · mol^{-1})[44,45]. All results are in accordance with its good thermal stability. Meanwhile, using the obtained E_i and $\ln A_i$ values, the Arrhenius equation can be expressed as $\ln k_{mm} = 41.31 - 186000/RT$ and $\ln k_{\mu m} = 41.56 - 186450/RT$ for the exothermic process, respectively, which can be applied to estimate the rate constants of the initial thermal decomposition processes.

Table 5 DSC data and calculated kinetic parameters of different sized crystals for **1**

β /K · min^{-1}	millimeter sized crystals (about 0.1 mm)						millimeter sized crystals (about 5 μm)					
	Kissinger				Ozawa		Kissinger				Ozawa	
	T_{p1} /K	E_K /kJ · mol^{-1}	$\ln A_K$	r	E_O /kJ · mol^{-1}	r	T_{p1} /K	E_K /kJ · mol^{-1}	$\ln A_K$	r	E_O /kJ · mol^{-1}	r
5	530.3						528.9					
10	538.9	186.3	41.34	0.9999	185.7	0.9997	537.3	186.8	41.56	0.9999	186.1	0.9999
15	543.9						542.3					
20	547.4						545.9					

3.5 Detonotion parameters

The detonation performance of a high explosive is characterized by its detonation velocity and detonation pressure. The empirical Kamlet—Jacobs equations [eqn. (3) and eqn. (4)] were employed to estimate the values of D and p [32,46].

$$D = 1.01(N\overline{M}^{1/2}Q^{1/2})^{1/2}(1+1.3\rho) \quad (3)$$

$$p = 1.558\rho^2 N\overline{M}^{1/2}Q^{1/2} \quad (4)$$

Where N is moles of gas detonation products per gram of explosive, mol · g^{-1}; $\overline{M}$ is average molecular mass of gaseous products, g · mol^{-1}; Q is chemical energy of detonation, kJ · g^{-1}; ρ is the density, g · cm^{-3}. The Q value should be calculated first to the D and p values. Q is also determined by the ΔH_f of the detonation reactant and product.

Here, the parameters N, $\overline{M}$, and Q were calculated according to eqns. (5), (6) and (7), respectively.

$$N = (b+d)/2M \quad (5)$$

$$\overline{M} = (2b+28d+32c)/(b+d) \quad (6)$$

$$Q = (57.8c+0.239\Delta H_f)/M \quad (7)$$

According to the Born-Haber energy cycle[47-48] (Fig. 10), the heat of formation of a salt can be simplified by eqn. (8):

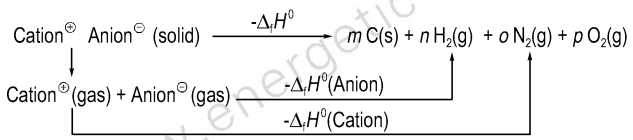

Fig. 10 Born-Haber cycle for the formation of energetic salts

The heats of formation of the cations and anions are obtained in our previous report[32]. The values of them are 875.1 kJ · mol^{-1} and −66.4 kJ · mol^{-1}, respectively. According to eqn. (3) to eqn. (7), the theoretically computed detonation velocity (D) is 7.9 km · s^{-1} and detonation pressure (p) is 26.5 GPa. This exhibits superior detonation performance than that of TNT (6881 m · s^{-1}, 19.50 GPa)[32].

Sensitivity deserves significant attention by researchers because it is closely linked with the safety of handling and applying explosives. In this study, impact sensitivities of the compounds were determined using the fall hammer test with approximately 50 mg samples (5.0 kg drop hammer), and found that the impact sensitivity of **1** was more than 60 J, which is possibly caused by the tautomerism of *s*-triazines ring to strengthen the bonds in the anions. The impact sensitivity of **1** is more insensitive than that of RDX (7.4 J)[27], HMX[27] and TNT (15 J)[32], even better than that of TATB (50 J)[32]. As is the case for the very insensitive explosive TATB, this salt can significantly improve the safety and survivability of munitions, weapons, and personnel, in addition to their quality explosive properties.

4 Conclusions

(1) A new energetic salt—triaminoguanidinium 2,4,6-trioxo-1,3,5-triazinan-1-ide was synthesized with a yield of 91%, and the structure was determined by X-ray single-crystal diffraction and fully characterized by UV-Vis, FT-IR, ^{1}H NMR, mass spectrometry and elemental analysis.

(2) Thermal stability, non-isothermal decomposition reaction kinetics and decomposition process were determined based on DSC and TG-FTIR analysis. Results indicated that it exhibited excellent resistance to thermal decompositions of up to 538.9 K (10 K · min^{-1}) and the constituents of the thermal decomposition gas are ammonia, carbon monoxide, and N_2. Non-isothermal kinetics analysis reveals that the value of E (about 186 kJ · mol^{-1}) closes to that of CL-20 (about 190 kJ · mol^{-1}).

(3) The detonation velocity and detonation pressure calculated by the empirical Kamlet-Jacobs formula are

7.9 km·s^{-1} and 26.5 GPa, respectively. Although detonation properties are not good enough, its impact sensitivity (IS> 60 J) determined by a BAM fall hammer test is very excellent, which is even better than TATB (50 J) and can be classified as impact insensitive energetic material.

References:

[1] DONG Hai-shan. Development and countermeasures of high energy density materials[J]. *Chinese Journal of Energetic Materials*(*Hanneng Cailiao*), 2004(Suppl.): 1–11.

[2] ZHANG Qing-hua, Shreeve J.M. Energetic ionic liquids as explosives and propellant fuels: a new journey of ionic liquid chemistry[J]. *Chemical Reviews*, 2014, 114(20): 10527–10574.

[3] Talawar M B, Sivabalan R, Senthilkumar N, et al. Synthesis, characterization and thermal studies on furazan-and tetrazine-based high energy materials[J]. *Journal of Hazardous Materials*, 2004, 113(1): 11–25.

[4] Hiskey M A, Goldman N, Stine J R. High-nitrogen energetic materials derived from azotetrazolate[J]. *Journal of Energetic Materials*, 1998, 16(2-3): 119–127.

[5] ZHANG Jia-heng, Mitchell L A, Parrish D A, et al. Enforced layer-by-layer stacking of energetic salts towards high-performance insensitive energetic materials[J]. *Journal of the American Chemical Society*, 2015, 137(33): 10532–10535.

[6] Zeman S, Jungová M. Sensitivity and performance of energetic materials[J]. *Propellants, Explosives, Pyrotechnics*, 2016, 41(3): 426–451.

[7] Pagoria P. A comparison of the structure, synthesis, and properties of insensitive energetic compounds[J]. *Propellants, Explosives, Pyrotechnics*, 2016, 41(3): 452–469.

[8] YAO Yan-ru, CHEN Xiang, HU Yong-peng, et al. Synthesis, crystal structure and thermodynamic properties of 3-(3,5-dimethylpyrazol-1-yl)-6-(benzylmethylene) hydrazone-s-tetrazine[J]. *The Journal of Chemical Thermodynamics*, 2017, 104: 67–72.

[9] BI Fu-qiang, FAN Zhi-zhong, XU Cheng, et al. Review on insensitive non-metallic energetic ionic compounds of tetrazolate anions[J]. *Chinese Journal of Energetic Materials*(*Hanneng Cailiao*), 2012, 20(6): 805–811.

[10] Thottempudi V, Shreeve J M. Synthesis and promising properties of a new family of high-density energetic salts of 5-nitro-3-trinitromethyl-1*H*-1,2,4-triazole and 5,5′-bis(trinitromethyl)-3,3′-azo-1*H*-1,2,4-triazole[J]. *Journal of the American Chemical Society*, 2011, 133(49): 19982–19992.

[11] GAO Hai-xiang, Shreeve J M. Azole-based energetic salts[J]. *Chemical Reviews*, 2011, 111(11): 7377–7436.

[12] Go bel M, Karaghiosoff K, Klapo tke T M, et al. Nitrotetrazolate-2*N*-oxides and the strategy of *N*-oxide introduction[J]. *Journal of the American Chemical Society*, 2010, 132(48): 17216–17226.

[13] Joo Y H, Shreeve J M. High-density energetic mono- or bis(oxy)-5-nitroiminotetrazoles[J]. *Angewandte Chemie International Edition*, 2010, 49(40): 7320–7323.

[14] Fischer D, Klapötke T M, Stierstorfer J. 1,5-Di(nitramino) tetrazole: high sensitivity and superior explosive performance[J]. *Angewandte Chemie International Edition*, 2015, 54(35): 10299–10302.

[15] Fischer A, Antonietti M, Thomas A. Growth confined by the nitrogen source: synthesis of pure metal nitride nanoparticles in mesoporous graphitic carbon nitride[J]. *Advanced Materials*, 2007, 19(2): 264–267.

[16] Banert K, Joo Y H, Rüffer T, et al. The exciting chemistry of tetraazidomethane[J]. *Angewandte Chemie International Edition*, 2007, 46(7): 1168–1171.

[17] YIN Ping, Parrish D A, Shreeve J M. Bis(nitroamino-1,2,4-triazolates): *N*-bridging strategy toward insensitive energetic materials[J]. *Angewandte Chemie International Edition*, 2014, 53(47): 12889–12892.

[18] ZHANG Yan-qiang, Parrish D A, Shreeve J M. Derivatives of 5-nitro-1,2,3-2*H*-triazole—high performance energetic materials[J]. *Journal of Materials Chemistry A*, 2013, 1(3): 585–593.

[19] YIN Ping, ZHANG Qing-hua, ZHANG Jia-heng, et al. *N*-Trinitroethylamino functionalization of nitroimidazoles: a new strategy for high performance energetic materials[J]. *Journal of Materials Chemistry A*, 2013, 1(25): 7500–7510.

[20] YIN Ping, ZHANG Jia-heng, Shreeve J M, et al. Polynitro-substituted pyrazoles and triazoles as potential energetic materials and oxidizers[J]. *Journal of Materials Chemistry A*, 2014, 2(9): 3200–3208.

[21] Dippold A A, Klapötke T M. A study of dinitro-bis-1,2,4-triazole-1,1′-diol and derivatives: design of high-performance insensitive energetic materials by the introduction of *N*-oxides[J]. *Journal of the American Chemical Society*, 2013, 135(26): 9931–9938.

[22] Fischer N, Fischer D, Klapötke T M, et al. Pushing the limits of energetic materials—the synthesis and characterization of dihydroxylammonium 5,5′-bistetrazole-1,1′-diolate[J]. *Journal of Materials Chemistry*, 2012, 22(38): 20418–20422.

[23] Pepekin V I. Limiting detonation velocities and limiting propelling powers of organic explosives[J]. *Doklady Physical Chemistry*. 2007, 414(2): 159–161.

[24] HUANG Yan-gen, ZHANG Yan-qiang, Shreeve J M. Nitrogen-rich salts based on energetic nitroaminodiazido[1,3,5]triazine and guanazine[J]. *Chemistry-A European Journal*, 2011, 17(5): 1538–1546.

[25] Shastin A V, Godovikova T I, Korsunskii B L. Nucleophilic substitution reactions of 2,4,6-tris(trinitromethyl)-1,3,5-triazine. 3. reaction of 2,4,6-tris(trinitromethyl)-1,3,5-triazine with azides and hydrazine[J]. *Chemistry of Heterocyclic Compounds*, 2003, 39(3): 354–356.

[26] Joo Y H, Shreeve J M. 1-Substituted 5-aminotetrazoles: syntheses from CNN_3 with primary amines[J]. *Organic Letters*, 2008, 10(20): 4665–4667.

[27] Joo Y H, Shreeve J M. Energetic mono-, di-, and trisubstituted nitroiminotetrazoles[J]. *Angewandte Chemie International Edition*, 2009, 121(3): 572–575.

[28] Joo Y H, Shreeve J M. Energetic ethylene- and Propylene-bridged bis(nitroiminotetrazolate) salts[J]. *Chemistry—A European Journal*, 2009, 15(13): 3198–3203.

[29] Berlinck R G S, Burtoloso A C B, Kossuga M H, et al The chemistry and biology of organic guanidine derivatives[J]. *Natural Product Reports*, 2010, 27(12): 1871–1907.

[30] Saczewski F, Balewski L Biological activities of guanidine compounds[J]. *Expert Opinion on Therapeutic Patents*, 2009, 19(10): 1417–1448.

[31] Fischer N, Joas M, Klapo tke T M, et al. Transition metal complexes of 3-amino-1-nitroguanidine as laser ignitible primary explosives: structures and properties[J]. *Inorganic Chemistry*, 2013, 52(23): 13791-13802.
[32] LIU Qiang-qiang, JIN Bo, PENG Ru-fang, et al. Synthesis, characterization and properties of nitrogen-rich compounds based on cyanuric acid: a promising design in the development of new energetic materials[J]. *Journal of Materials Chemistry A*, 2016, 4(13): 4971-4981.
[33] Sheldrick G M. SHELXS-97 and SHELXL-97, Programs for the Solution and Refinement of Crystal Structures[CP]. University of Göttingen, Germany, 1997.
[34] Sheldrick G M. SHELXS-97-A program for automatic solution of crystal structures[CP]. University of Goettingen, Goettingen, Germany, 1997.
[35] Klapötke T M, Stierstorfer J. Triaminoguanidinium dinitramide—calculations, synthesis and characterization of a promising energetic compound[J]. *Physical Chemistry Chemical Physics*, 2008, 10(29): 4340-4346.
[37] WU Jin-ting, ZHANG Jian-guo, YIN Xin, et al. Synthesis and characterization of the nitrophenol energetic ionic salts of 5,6,7,8-Tetrahydrotetrazolo[1,5-b][1,2,4]triazine[J]. *European Journal of Inorganic Chemistry*, 2014, 2014(27): 4690-4695.
[38] Fischer D, Klapötke T M, Stierstorfer J. Salts of tetrazolone—synthesis and properties of insensitive energetic materials[J]. *Propellants, Explosives, Pyrotechnics*, 2012, 37(2): 156-166.
[39] LIU Qiang-qiang, JIN Bo, ZHANG Qing-chun, et al. Nitrogen-rich energetic metal-organic framework: synthesis, structure, properties, and thermal behaviors of Pb(Ⅱ) complex based on *N*,*N*-bis(1*H*-tetrazole-5-yl)-amine[J]. *Materials*, 2016, 9(8): 681.
[40] Cacho-Bailo F, Téllez C, Coronas J. Interactive thermal effects on metal—organic framework polymer composite membranes[J]. *Chemistry-A European Journal*, 2016, 22(28): 9533-9536.
[41] Kissinger H E. Reaction kinetics in differential thermal analysis[J]. *Analytical Chemistry*, 1957, 29(11): 1702-1706.
[42] Doyle C D. Kinetic analysis of thermogravimetric data[J]. *Journal of Applied Polymer Science*, 1961, 5(15): 285-292.
[43] Ozawa T. A new method of analyzing thermogravimetric data[J]. *Bulletin of the Chemical Society of Japan*, 1965, 38(11): 1881-1886.
[44] Geetha M, Nair U R, Sarwade D B, et al. Studies on CL-20: the most powerful high energy material[J]. *Journal of Thermal Analysis and Calorimetry*, 2003, 73(3): 913-922.
[45] Turcotte R, Vachon M, Kwok Q S M, et al. Thermal study of HNIW (CL-20)[J]. *Thermochimica Acta*, 2005, 433(1): 105-115.
[46] Chand D, Parrish D A, Shreeve J M. Di(1*H*-tetrazol-5-yl)methanone oxime and 5,5′-(hydrazonomethylene) bis(1*H*-tetrazole) and their salts: a family of highly useful new tetrazoles and energetic materials[J]. *Journal of Materials Chemistry A*, 2013, 1(48): 15383-15389.
[47] GAO Hai-xiang, YE Cheng-feng, Piekarski C M, et al. Computational characterization of energetic salts[J]. *The Journal of Physical Chemistry C*, 2007, 111(28): 10718-10731.
[48] Ghule V D. Computational screening of nitrogen-rich energetic salts based on substituted triazine[J]. *The Journal of Physical Chemistry C*, 2013, 117(33): 16840-16849.

三聚氰酸为基的2,4,6-三氧-[1,3,5]三嗪烷-1-三氨基胍盐的合成、晶体结构和热性能

刘强强[1,2], 金 波[2], 张青春[2], 尚 宇[2], 郭志成[3], 彭汝芳[1,2]
(1. 中国工程物理研究院激光聚变研究中心,四川 绵阳 621999; 2. 西南科技大学四川省非金属复合与功能材料重点实验室——省部共建国家重点实验室培育基地,四川 绵阳 621010; 3. 西南科技大学国防科技学院,四川 绵阳 621010)

摘 要: 以三聚氰酸钠(CANa)和三氨基胍盐酸盐(TAG-HCl)为原料,通过一步复分解反应制备了一种富氮含能化合物——2,4,6-三氧-[1,3,5]三嗪烷-1-三氨基胍盐(**1**),收率91%。采用X-射线单晶衍射、UV-Vis、FTIR、^{1}H NMR以及元素分析等对产物进行了结构表征。计算了产物的生成焓和爆轰参数。通过差示扫描量热法(DSC,10 K·min^{-1})和热重-傅里叶变换红外光谱联用分析了其热稳定性、非等温热分解动力学和热分解过程。通过落锤法测试了产物的撞击感度。结果表明,化合物**1**的晶体为单斜晶系,$P2_1/n$空间群,计算密度为1.676 g·cm^{-3},生成焓为327.9 kJ·mol^{-1},爆速为7900 m·s^{-1},爆压为26.5 GPa。化合物具**1**有良好的热稳定性,分解峰值温度为538.9 K,提出了N_2气氛下可能的热分解机理。且化合物**1**对撞击非常钝感,撞击感度大于60 J,优于TATB(50 J)。

关键词: 2,4,6-三氧-[1,3,5]三嗪烷-1-三氨基胍盐; 三聚氰酸; 离子盐; 单晶结构; 动力学; 热分解
中图分类号: TJ55; O62 **文献标志码:** A **DOI:** 10.11943/j.issn.1006-9941.2017.10.007